Spectroscopic and Equilibrium Dialysis Studies of the Poly(acrylic acid)-Cu(II) Complex in the pH Range 3.5—7[1)]

Kiwamu YAMAOKA* and Tsutomu MASUJIMA
Faculty of Science, Hiroshima University, Higashisenda-machi, Hiroshima 730

(Received December 25, 1978)

The complex formation between poly(acrylic acid), poly(Acr), and Cu^{2+} ion was studied in 150 mM NaCl solutions at 25 °C and at the mixing ratios of Acr residues-to-Cu^{2+}, R, of 32, 16 and 8, in the pH range of 3.5—7 by the spectroscopic and equilibrium dialysis methods. The dialysis results showed that more than 90% of the Cu^{2+} ions remain bound to the polymer at pH's higher than 4.5, but the bound Cu(II) begins to dissociate at lower pH values. The data also revealed that the true absorption spectra of poly(Acr)–Cu(II) complexes varied with pH and R in a complicated manner. The analysis of the bound Cu(II) spectra disclosed the presence of three different kinds of Cu(II)–Acr complexes over the entire pH range. It is the relative amounts of these three complexes that vary with pH and R. With a newly devised plot of the dialysis data, the stability constant for each Cu(II)–Acr complex was determined. In the poly(Acr)–Cu(II) macrocomplex, each Cu(II) was estimated to bind to two or four carboxylato ligands.

In a previous investigation in which the complex formation of poly(α-L-glutamic acid), poly(Glu), with Cu^{2+} was studied in the pH range between 7 and 3, poly(acrylic acid), poly(Acr), was chosen as the polymeric model of poly(Glu).[2)] The absorption spectra of poly(Glu)- and poly(Acr)–Cu(II) systems were both found to vary with pH in an unexpectedly complicated manner, but their pH dependence differed from each other. The finding was qualitatively attributed to the difference in the conformational change between poly(Glu) and poly(Acr) to which Cu(II) is bound, and also to the fact that the peptide nitrogen, a likely ligand to Cu(II), is lacking in the poly(Acr) residue. The finding also indicated that Cu(II)-residue complexes of various types are present in each polyanion–Cu(II) system. It is thus quite significant to study the structural details of poly(Glu)- and poly(Acr)–Cu(II) complexes by analyzing their absorption spectra quantitatively.

Spectroscopic and structural studies of the poly(Acr)–Cu(II) system in solutions are numerous;[2–10)] however, some conflicting views have been given on the nature of the binding of Cu(II) to poly(Acr). For example, the pH variation of the absorption intensity was attributed either to the conformational change of the macromolecular complex[3)] or to the change in the amount of bound Cu(II).[8)] Two binding schemes between Cu^{2+} and the side-chain carboxylato groups of poly(Acr) have been presented: Cu(II) binds to two adjacent[3,7)] or distant[8)] carboxylato groups. In addition, the number of the ligands participating in the complex formation has been suggested to be either two carboxylato groups[3,7–10)] or more than two,[4)] or both depending on the conditions.[6)] The same points of controversy have also been noted in the reports on the poly(methacrylic acid)–Cu(II) complex.[4,5,11–16)]

In order to clarify those unresolved questions, the visible-UV absorption spectra of poly(Acr)–Cu(II) solutions were measured in the pH range 7—3.5. The concentration and the molar absorption coefficient of the *bound* Cu(II), ε^b, were directly determined by the equilibrium dialysis method. The ε^b values vary in a complicated way, but systematically depend on both pH and the mixing ratio of Acr residues-to-Cu^{2+} ion. The ε^b *vs.* pH curves could be explained reasonably well as the interplay of three limiting spectra which characterize three types of Cu(II)–Acr complexes in poly(Acr). The binding schemes between Cu^{2+} and poly(Acr), the dissociation constants of poly(Acr), and the stability constants of poly(Acr)–Cu(II) complexes were also determined by means of graphical plots. The schemes of two and four side-chain carboxylato groups bound by a Cu(II) are sufficient to explain the binding data. By comparing those new data with the spectra of such low molecular weight models as the glutaric acid- and malonic acid–Cu(II) complexes, the nature of the poly(Acr)–Cu(II) complex will be discussed.

Experimental

Materials. Poly(sodium acrylate), abbreviated simply as poly(Acr), was purchased from Nakarai Chemical Co., Kyoto, and purified from an aqueous solution by means of dialysis against redistilled water for 24 h. The sample solution was freeze-dried and then vacuum-dried at 56 °C for 7 h. The degree of polymerization was determined to be *ca.* 7700 from the intrinsic viscosity in 1 M (=mol dm^{-3}) NaCl.[17)] Reagent grade copper(II) chloride dihydrate was crystallized from redistilled water before use. All other chemicals were of reagent grade and used without further purification.

Preparation of Sample Solutions. Each of the NaCl, $CuCl_2$, and HCl solutions was added to a stock polymer solution in this order. In every poly(Acr)–Cu(II) solution, the concentration of the polymer and the total of the concentrations of HCl and NaCl were always kept constant at 8 mM and 150 mM, respectively. The mixing ratio, R, defined as the mean residue weight concentration of Acr residues to the total concentration of Cu^{2+} in the sample solution, was adjusted by changing the initial Cu^{2+} concentration. The pH of the sample solution was adjusted by the addition of 0.125 M HCl.

Equilibrium Dialysis. The procedures and device for equilibrium dialysis were described elsewhere.[18)] The volumes of the two chambers of the dialysis cell were designed to be *ca.* 14 and 3.5 ml. The poly(Acr)–Cu(II) solution (13 ml) and the 150 mM NaCl solution (3.3 ml) were filled in the larger and smaller chambers, respectively, in order to minimize the changes in both R and pH of the poly(Acr)–Cu(II) solution during dialysis. The assembled dialysis cells were rotated continuously for 45 h at 15 rpm and at 25 °C. A period of 24 h was sufficient for a Cu^{2+} solution to reach a complete equilibrium. The adsorption of Cu^{2+} on the dialysis membrane was negligible. When the dialysis was completed, the absorption spectra and pH of the sample solution in the larger cell chamber were measured in sequence. The colorimetric determination of unbound Cu^{2+} ions in the smaller chamber was carried out as described below.

Colorimetric Determination of Cu^{2+} Ions. 2,2′-Biquinoline (Merck Co., Ltd.) was used as a chelating agent to determine the Cu^{2+} concentration. The procedure for this colorimetry is given in Merck Cat. No. 2955. A molar absorption coefficient of 5780 at 546 nm was used for the chelated Cu(II). The calibration curve obeyed Beer's law up to 15 μM of Cu^{2+}. With the concentration of the unbound Cu^{2+}, $[\mathrm{Cu}]_f$, thus determined from the dialysate, the concentration of the bound Cu(II) in the dialyzed poly(Acr)–Cu(II) solution, $[\mathrm{Cu}]_b$, was calculated as:

$$[\mathrm{Cu}]_b = [\mathrm{Cu}]_0 - [\mathrm{Cu}]_f \frac{(V_1+V_2)}{V_1}, \qquad (1)$$

where $[\mathrm{Cu}]_0$ is the initial concentration of Cu^{2+} in the poly(Acr)–Cu(II) solution; V_1 and V_2 are the initial volumes of the poly(Acr)–Cu(II) and 150 mM NaCl solutions, respectively. The volume change in the poly(Acr)–Cu(II) solution before and after dialysis was *ca.* 1.5 % at most, even in the high pH and R range where the Donnan effect could possibly be appreciable. Thus, the Donnan effect should be negligible under the present experimental conditions. The binding fraction of Cu(II), f_b, is obtained as follows:

$$f_b = \frac{[\mathrm{Cu}]_b}{[\mathrm{Cu}]_b + [\mathrm{Cu}]_f}. \qquad (2)$$

Measurements of Absorption Spectra and pH. The absorption spectra and pH of sample solutions were measured as described elsewhere.[2)] The pH calibration was made against the standard pH solutions (pH 6.88 and 4.00). All experiments were carried out at 25±1 °C.

Results

Absorption Spectra of Poly(Acr)–Cu(II) Solutions. The absorption spectra of poly(Acr)–Cu(II) solutions at various pH and R are shown in Fig. 1. The spectra are characterized by three new bands: a peak at 250—260 nm ($\varepsilon \leq 5000$), a weak shoulder near 370 nm ($\varepsilon \leq 40$), and a peak at 680—710 nm ($40 \leq \varepsilon \leq 120$). These bands are denoted as the UV-, near UV-, and visible bands from the short wavelength end. The spectrum of the $\mathrm{CuCl_2}$ solution in 150 mM NaCl (pH 3.45—5.74) shows a shoulder near 250 nm ($\varepsilon \approx 230$) and a weak peak near 800 nm ($\varepsilon \approx 13$) (Fig. 1(a)). The spectrum of the poly(Acr) solution in 150 mM NaCl also shows only an ascending curve below 250 nm (Figs. 1(a)—(c)). The new three bands clearly reflect the formation of the poly(Acr)–Cu(II) complex. However, no isosbestic point was observed in either band in the pH range 4—7.

The spectra of poly(Acr)–Cu(II) solutions vary in a complicated manner depending on pH and R. In Fig. 2, the apparent molar absorption coefficients, ε_λ, at 250 and 710 nm are plotted against pH. The wavelengths are close to the peaks of the UV- and visible bands, respectively. The ε values at the two wavelengths vary differently in the pH range 6.5—4.3. As the pH is lowered from 6, the visible band intensity increases and reaches a maximum at a pH of 4.4—4.3, while the UV-band intensity remains almost unchanged. At the pH lower than 4.3, however, all of the ε *vs.* pH curves descend monotonically.

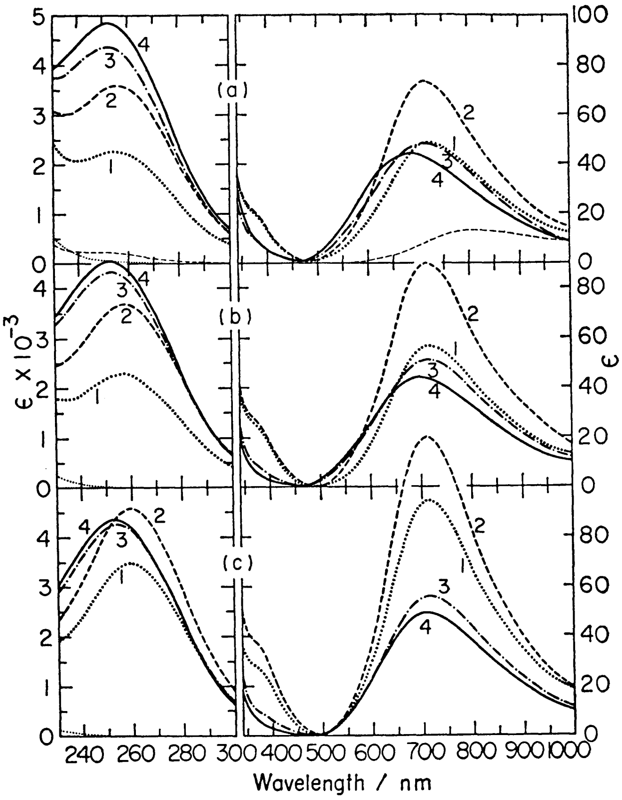

Fig. 1. The UV and visible absorption spectra of Cu^{2+} in the presence of poly(Acr) in 150 mM NaCl at various pH. (a): $R=32$; pH=3.85 (1), 4.11 (2), 5.50 (3), and 6.60 (4). (b): $R=16$; pH=3.90 (1), 4.17 (2), 5.87 (3), and 6.51 (4). (c): $R=8$; pH=3.94 (1), 4.21 (2), 6.09 (3), and 6.42 (4). The numeral in the parentheses corresponds to the numbered spectrum. The molar absorption coefficient, ε, is expressed in terms of the total concentration of Cu^{2+} present in solution. The dotted curves (without number) in the UV region are the spectra of poly(Acr) expressed in terms of $\varepsilon \cdot R$. The spectra of $\mathrm{CuCl_2}$ solutions are constant in the pH range 3.54—5.74. An example is given in (a) (—— without number).

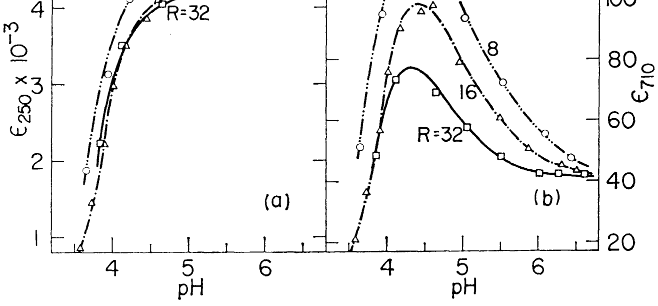

Fig. 2. The variation of the molar absorption coefficients of Cu^{2+}, ε, with pH in the presence of poly(Acr) at various R and at selected wavelengths of (a) 250 nm and (b) 710 nm.

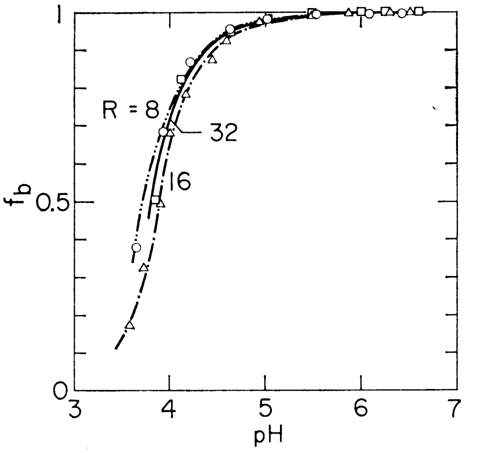

Fig. 3. The variation of the binding fraction of Cu(II), f_b, with pH at various R.

The Binding Fraction of Cu^{2+} *and Its Variation with* pH. In order to express the pH dependence of the absorption intensity in terms of the amount of the *bound* Cu(II), the binding fraction, f_b, was estimated from the dialysis data with the aid of Eq. 2. The results are shown in Fig. 3. Almost all the Cu^{2+} ions added in the poly(Acr) are bound to the polymer at pH values higher than 5.5, and more than 90% of the total Cu^{2+} indeed remain bound in the pH range 5.5—4.5. The bound Cu(II) begins to dissociate from the polymer site with the further decrease in pH. Only at a pH lower than 4.5 do the f_b *vs*. pH curves behave similarly to the ε *vs*. pH curves (*cf*. Fig. 2). These dialysis results show that the variation in ε at a pH higher than 4.5 is not due to the change of the amount of the bound Cu(II), but to the change in the ε of the bound Cu(II) itself.

The pH *Dependence of the Molar Absorption Coefficient and the Peak Position of the Bound Cu(II)*. Since the bound and unbound Cu^{2+} concentrations are now available, the molar absorption coefficient of the *bound* Cu(II), ε^b, can be determined by using f_b in the following equation:

$$\varepsilon_\lambda^b = \frac{1}{f_b}(\varepsilon_\lambda - \varepsilon_\lambda^f) - \frac{[Cu]_0}{[Cu]_b} R\cdot\varepsilon_\lambda^p + \varepsilon_\lambda^f, \qquad (3)$$

where ε_λ, ε_λ^p, and ε_λ^f are the molar absorption coefficients at wavelength λ of the poly(Acr)–Cu(II), poly(Acr), and unbound Cu^{2+} in 150 mM NaCl solutions, respectively. The ε^b values are evaluated at four wavelengths: 250 and 710 nm (near the peaks of UV- and visible bands), 370 nm (the shoulder of near UV-band), and 880 nm (a hump of the visible band). The results are shown in Figs. 4(a)—(d), together with the peak wavelengths of the UV- and visible bands, denoted as λ_{max}, in Figs. 4(e) and (f). It should be noted that these ε^b *vs*. pH curves demonstrate the real changes in the optical property of the *bound* Cu(II) in poly(Acr)–Cu(II).

The ε_{250}^b *vs*. pH curves are peculiar in that they show a U-type change (Fig. 4(a)). On the other hand, the ε_{710}^b and ε_{880}^b curves are sigmoidal (Figs. 4(b) and (d)). In both sets of these curves, however, the ε^b converges to the limiting ε^b values on the high and low pH sides, as indicated by broken lines I and III. The limiting ε_{250}^b values are 4800 (pH≥6.8 and R=32) and 4950 (pH≤3.6 and R=8) in Fig. 4(a), while the limiting ε_{710}^b and ε_{880}^b values are 40 and 19 (pH≥6.8 and R=32), and 150 and 60 (pH≤3.6 and R=8) in Figs. 4(b) and (d), respectively. The minimum points in the ε_{250}^b *vs*. pH curves yield a constant value of 4250 regardless of R (pH=5.0 and R=32, pH=5.5 and R=16, and pH=5.9 and R=8), as indicated by broken line II in Fig. 4(a). Interestingly, the ε_{710}^b and ε_{880}^b values are also constant regardless of R at these respective pH values, becoming 60 and 28 respectively, as indicated by broken line II in Figs. 4(b) and (d).

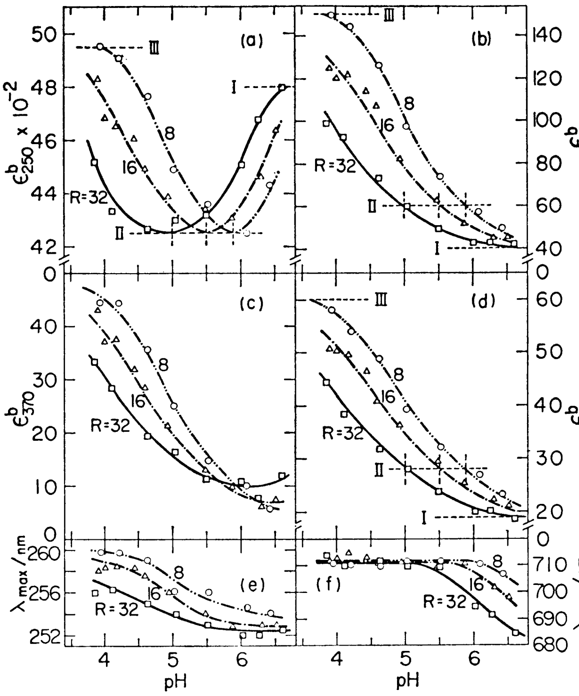

Fig. 4. The pH variation of the absorption coefficients of bound Cu(II), ε^b, at selected wavelengths of (a) 250 nm, (b) 710 nm, (c) 370 nm, and (d) 880 nm, and the variation of the peak positions of (e) the UV- and (f) visible-bands, λ_{max}. The ε^b and λ_{max} were estimated by applying Eq. 3 to each absorption spectrum of poly(Acr)–Cu(II) solution. The broken lines in (a), (b), and (d) show the characteristic values of ε^b at three pH regions of I, II, and III.

Concurrently with the changes in ε^b, the peak positions, λ_{max}, in the spectra of bound Cu(II) vary with pH in two steps, as shown in Figs. 4(e) and (f). The λ_{max} of the UV-band is almost constant (252.5 nm (R=32), 253 nm (R=16), and 254 nm (R=8)) in the

TABLE 1. THE MOLAR ABSORPTION COEFFICIENTS, ε_λ^b IN $cm^{-1}\cdot mol^{-1}\cdot dm^3$, AND THE PEAK POSITIONS, λ_{max} IN nm, IN THE SPECTRA OF Cu(II) BOUND TO poly(Acr) IN THREE pH REGIONS I, II, AND III

pH	ε_{250}^b	λ_{max}	ε_{710}^b	ε_{880}^b	λ_{max}
I	4800	252.5—253.5	40	19	685
II	4250	254.0—254.5	60	28	710—713
III	4950	260	150	60	710—713

pH range between 6.8 and 5.9—5.5, where the ε_{250}^b values are lowest, and then begins to shift to *ca.* 260 nm with the further lowering of pH. On the other hand, the λ_{max} of the visible band varies from 685 nm (R=32 at pH=6.8) to near 711 nm and remains constant in the lower pH range (pH≤5.0). These data are summarized in Table 1. The two-step change of the respective absorption peaks of the visible and UV-bands for the bound Cu(II) suggests the presence of two or three kinds of the Cu(II)–Acr complexes in poly(Acr)–Cu(II).

Assignment of ε^b*-Values to the Three Complexes.* The complicated variations of the ε_λ^b of bound Cu(II) with pH in Fig. 4 can be best explained as an interplay of three limiting ε_λ^b-values over the entire pH range under consideration of the data given in the preceding section. These limiting ε_λ^b-values may then be either characteristic of three different chemical species of the Cu(II)–Acr complexes or representative of three different states of a single or a mixture of Cu(II)–Acr complex(es) formed in poly(Acr)–Cu(II).

On the assumption that three limiting values of ε_λ^b in Table 1 specify three structurally different Cu(II)–Acr complexes, which are denoted as complexes I, II, and III, the fraction of each complex i (i=I, II, III) to the total of the bound Cu(II), f_I, f_{II}, and f_{III}, may be calculated at a given pH and at a selected wavelength of λ as follows:

$$\varepsilon_\lambda^b = \sum_{i=I}^{III} f_i(\varepsilon_\lambda^b)_i \text{ and } \sum_{i=I}^{III} f_i = 1, \tag{4}$$

where $(\varepsilon_\lambda^b)_i$ is the ε_λ^b-value characteristic of complex i. With the values of $(\varepsilon_\lambda^b)_i$ at 250 and 710 nm in Table 1, Eq. 4 can be written explicitly as follows:

$$\begin{aligned} \varepsilon_{250}^b &= 4800f_I + 4250f_{II} + 4950f_{III}, \\ \varepsilon_{710}^b &= 40f_I + 60f_{II} + 150f_{III}, \text{ and } f_I + f_{II} + f_{III} = 1. \end{aligned} \tag{5}$$

By solving these simultaneous equations for f_I, f_{II}, and f_{III} with the observed ε_{250}^b and ε_{710}^b at given pH and R values, the pH dependence of the f_i's may be obtained.

Figure 5 shows the variation of the fraction of complex i, f_i, with pH at three different R. At R=32 (Fig. 5(a)), complex I is dominant at high pH(≥6.1) and then its fraction decreases on lowering the pH. Simultaneously, the fraction of complex II, f_{II}, increases to unity at pH=5 and then decreases in the lower pH range where complex III now becomes dominant. With decrease in R (Figs. 5(b) and (c)), the f_i *vs.* pH curves shift to the high pH region as compared with the curves for R=32. These shifts may result from the lowering of the degree of dissociation, $\alpha^\bullet$, of the side-chain carboxylato groups by the binding of Cu(II) even at the same pH. In order to test this hypothesis, the pH should be converted into the $\alpha^\bullet$, which is defined as

$$\alpha^\bullet = 1 - \frac{[\mathrm{HCl}]_{\mathrm{add}} + 2[\mathrm{Cu}]_{\mathrm{b}}}{[\mathrm{Acr}]_0}, \tag{6}$$

where $[\mathrm{Acr}]_0$ is the initial residue concentration of poly(Acr), and $[\mathrm{HCl}]_{\mathrm{add}}$ is the concentration of HCl added to the solution.

The dependence of f_i on $\alpha^\bullet$ is shown in Fig. 5(d). The f_i *vs.* $\alpha^\bullet$ curves at three R do not coincide with one another in this plot. Thus the horizontal displacement of the f_i toward higher pH is not due solely to the neutralization of the carboxylato group by Cu(II) but due also to the change in the ε^b of the bound Cu(II) with R. In any case, complex II is most dominant when about half of the carboxyl groups of poly(Acr) are ionized, while complexes I and III become a major entity in the fully ionized and un-ionized conformations of poly(Acr)–Cu(II), respectively. Accordingly, the pH region may also be divided into three subregions, *i.e.*, pH regions I, II, and III.

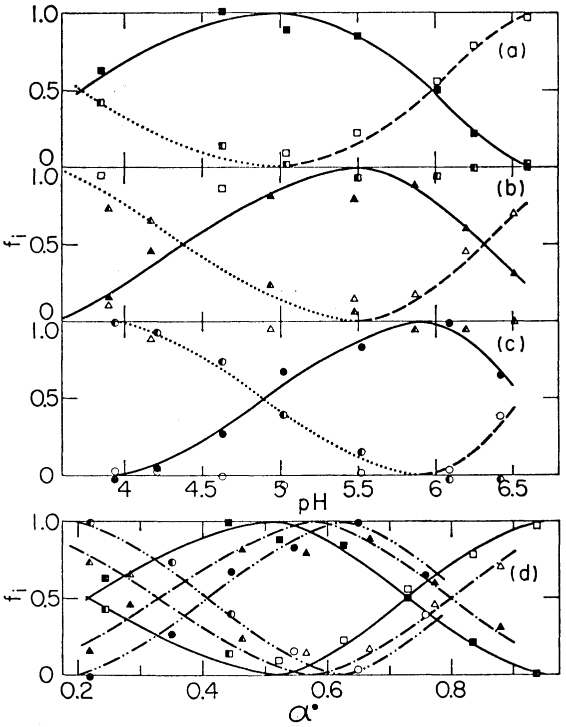

Fig. 5. The pH dependence of the fraction of the Cu(II)–Acr complex i (i=I, II, and III) to the total bound Cu(II), f_i, at various R; (a) R=32, (b) 16, and (c) 8; Complex I (---- and open symbols), complex II (—— and filled symbols), and complex III (······ and half-filled symbols), together with the variation of the f_i with the degree of dissociation of poly(Acr), $\alpha^\bullet$, at various R (32 —, 16 -·, 8 -··) in (d).

Component Spectra of the Bound Cu(II) in Poly(Acr)–Cu(II). Since the overall spectrum of the bound Cu(II) in the poly(Acr)–Cu(II) could be obtained in terms of ε_λ^b (Eq. 3), it is now possible to divide it into three component spectra characteristic of complexes I, II, and III by using the results shown in Fig. 5. For the poly(Acr)–Cu(II) at a given R (=32, 16 or 8), the pH-independent component spectra can be calculated from Eq. 4 first by solving simultaneous equations for $(\varepsilon_\lambda^b)_I$, $(\varepsilon_\lambda^b)_{II}$, and $(\varepsilon_\lambda^b)_{III}$ at a wavelength of λ with both ε_λ^b- and f_i-values at any three pH, and then by repeating the same calculations at other wavelengths in the 940—230 nm regions. Several of those spectra were derived by employing the data at different sets of three pH values and averaged. The mean spectra were designated as component spectra I, II, and III for complexes I, II, and III at a given R. The results are shown for the visible and UV-bands in Fig. 6. It should be noted that each of the component spectra is

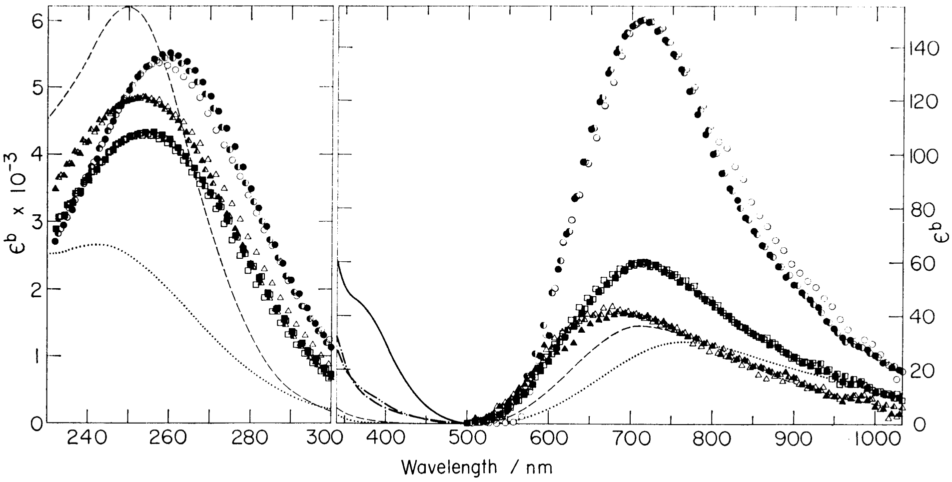

Fig. 6. The spectra of complexes I, II, and III in poly(Acr)–Cu(II). Complex I: $R=32$ (△), 16 (◭), and 8 (▲). Complex II: $R=32$ (□), 16 (◧), and 8 (■). Complex III: $R=32$ (○), 16 (◐), and 8 (●). For the procedure of the determination of these spectra, see text. This procedure could not be applied to the near UV-band because of the low absorption intensity. Instead, some typical spectra, which are closest to $f_{\mathrm{i}}=1$, are shown (Complex I –·–, Complex II –··–, and Complex III ——). The spectra of Cu(II)–glutarate (······) and -malonate (––––) complexes ($R=$[carboxyl group]/$[\mathrm{Cu}^{2+}]_0=80$) are also shown for comparison.

nearly independent of the R and pH values. It is component spectrum III, which represents the dominant complex in the low pH region, that is most intense in the visible wavelength and gives rise to a considerable shoulder in the near UV-band. Although component spectra II and III both show the peak of the visible band at the same wavelength of 710 nm, they differ from each other in that II is weaker but broader than III.

The spectra of the bound Cu(II) in the glutaric acid- and malonic acid–Cu(II) complexes are also shown in Fig. 6 for comparison. Glutaric acid was chosen as the model for the nearest neighbor ligands of poly(Acr), because it has the same number of carbon atoms between two carboxylato groups. Malonic acid is known to form a four-coordinated complex with Cu(II) at the high carboxylate-to-Cu(II) ratio.[19] The spectra of the glutaric acid–Cu(II) complex with the R values up to 60 never resemble any of those component spectra I, II, and III as regards the peak position and intensity. However, the spectra of malonic acid–Cu(II) complexes at high R are quite similar to component spectrum II of the Cu(II)–Acr complex in the poly(Acr)–Cu(II) as regards the general spectral features in the visible band. This similarity is suggestive of the structure of complex II.

Formation of Cu(II)–Acr Complexes in Poly(Acr)–Cu(II). The structure of the Cu(II)–Acr complex may be reflected in the stoichiometry of the complex formation between the Acr residue and Cu^{2+}. On the basis that the equilibrium constant depends inversely on the first power of $[\mathrm{Acr}]_0$, Wall and Gill[3] have concluded that a pair of the intramolecular adjacent carboxylato groups is chelated with a Cu(II). On the other hand, Tamaoki *et al.*[8] considered that two carboxyl ligands separated from each other on a single polyanion are associated with a Cu(II), because the Cu(II) showed almost the same binding strength for polycarboxylates of varying tacticities. In order to clarify the binding process between Cu^{2+} and poly(Acr) from the equilibrium dialysis data, some graphical methods were devised.

The following equilibrium schemes are considered for the binding between Cu^{2+} and carboxylato ligands of poly(Acr).

$$\text{Scheme A: } \mathrm{COOH} \overset{K_1}{\rightleftharpoons} \mathrm{COO^-} + \mathrm{H^+},$$

$$(\mathrm{COO^-})_2 + \mathrm{Cu^{2+}} \overset{K_2}{\rightleftharpoons} (\mathrm{COO})_2\mathrm{Cu}. \quad (7)$$

$$\text{Scheme B: } \mathrm{COOH} \overset{K_1}{\rightleftharpoons} \mathrm{COO^-} + \mathrm{H^+},$$

$$2(\mathrm{COO^-}) + \mathrm{Cu^{2+}} \overset{K_3}{\rightleftharpoons} \mathrm{COOCuOOC}. \quad (8)$$

In these schemes, the K_1, K_2, and K_3 are the dissociation constant of poly(Acr) and the stability constants of two different Cu(II)-residue complexes and are given as

$$K_1 = \frac{[\mathrm{COO^-}][\mathrm{H^+}]}{[\mathrm{COOH}]}, \quad (9)$$

$$K_2 = \frac{[(\mathrm{COO})_2\mathrm{Cu}]}{[(\mathrm{COO^-})_2][\mathrm{Cu^{2+}}]}, \quad (10)$$

and

$$K_3 = \frac{[\mathrm{COOCuOOC}]}{[\mathrm{COO^-}]^2[\mathrm{Cu^{2+}}]}. \quad (11)$$

In Scheme A, a Cu^{2+} ion binds to two adjacent carboxylato groups, whereas in Scheme B it binds to any two carboxylato groups. All the values of K_1, K_2, and K_3 are only apparent, since they are expressed in terms of concentrations and include the contribution of the electrostatic potential field of the polyanion. The total concentration of the ligands of poly(Acr) is given as

$$P_0 \equiv [\mathrm{Acr}]_0 = [\mathrm{COO^-}] + [\mathrm{COOH}] + 2[(\mathrm{COO})_2\mathrm{Cu}]. \quad (12)$$

The concentration of the pairs of nearest-neighbor carboxylato groups in poly(Acr), $[(\mathrm{COO}^-)_2]$, may be given as:

$$[(\mathrm{COO}^-)_2] = q[\mathrm{COO}^-]. \tag{13}$$

Equations 9, 10, 12, and 13 are combined for Scheme A:

$$\frac{q(P_0-2\beta)}{\sigma} = \frac{[\mathrm{H}^+]}{K_1K_2} + \frac{1}{K_2}, \tag{14}$$

or

$$\log\left(\frac{q(P_0-2\beta)K_2}{\sigma} - 1\right) = -\mathrm{pH} + \mathrm{p}K_1. \tag{15}$$

Equations 9, 11, and 12 are combined for Scheme B:

$$\frac{P_0-2\beta}{\sqrt{\sigma}} = \frac{[\mathrm{H}^+]}{K_1\sqrt{K_3}} + \frac{1}{\sqrt{K_3}}, \tag{16}$$

or

$$\log\left(\frac{(P_0-2\beta)\sqrt{K_3}}{\sqrt{\sigma}} - 1\right) = -\mathrm{pH} + \mathrm{p}K_1, \tag{17}$$

where β is the concentration of bound Cu(II) or Cu(II)–Acr complex, and σ is the ratio of the concentration of the bound Cu(II) to that of unbound Cu^{2+}. The quantities P_0, β, σ, and $[\mathrm{H}^+]$ are all obtained experimentally. When the left-hand side of Eq. 14 or 16 is plotted against $[\mathrm{H}^+]$, a straight line would result, provided that the complex formation occurs according to Scheme A or B. The intercept and tangent of this line give the K_2 or K_3 together with K_1. The results are shown in Fig. 7, where the value of q is assumed to be 0.5.[3] Alternatively, Eqs. 15 and 17 may be utilized, in the cases where the intercepts are too small to estimate K_1, K_2, and K_3 unambiguously. With a number of assumed K_2 and K_3 values, the left-hand side of Eq. 15 or 17 is plotted against pH, until a straight line with a slope of -1 is obtained. Then the assumed K_2 or K_3 is the desired value and, in this case, the pK_1 is equal to the pH at which the straight line crosses the abscissa. The results are shown in Fig. 8.

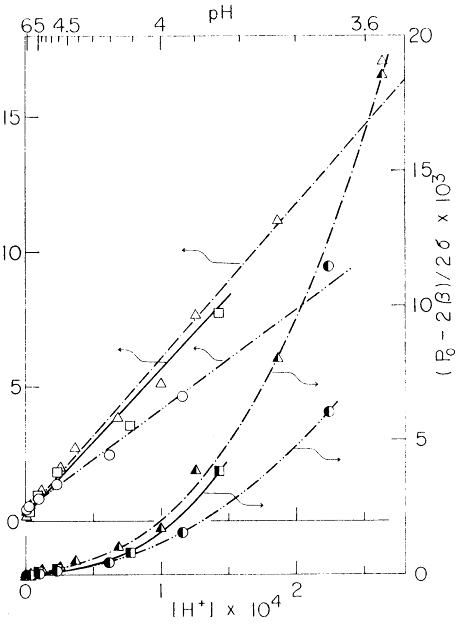

Fig. 7. The binding plots at three R for Scheme A (the right ordinate) and for Scheme B (the left ordinate). R=32 (◧ and □), 16 (▲ and △), and 8 (◐ and ○). See text for other details.

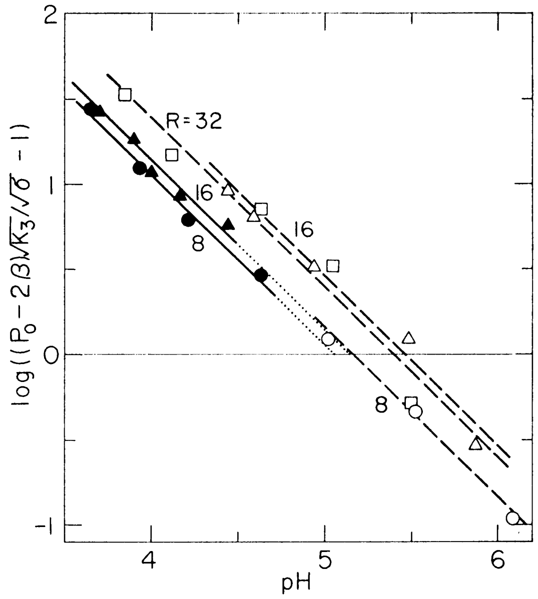

Fig. 8. The logarithmic binding plot at various R for Scheme B in pH regions II (open symbols) and III (filled symbols). The straight lines are best fitted by the f_i-weighted least-squares method. See text for other details.

If Scheme A describes the complex formation between Cu^{2+} and Acr ligands in all three pH regions I, II, and III, the above plot (Eq. 14) should give rise to a straight line over an entire range of $[\mathrm{H}^+]$. This is not the case, as is demonstrated in Fig. 7. Scheme A may tentatively be concluded not to describe adequately the complex formation in the lower pH regions II and III, at least, under the assumption that the concentration of the adjacent two carboxylato groups is proportional to the concentration of the side-chain carboxylato groups remaining on poly(Acr),[3] *i.e.*, q is constant in Eq. 13. However, the validity of this assumption is believed open to further investigations. On the other hand, Scheme B is adequate to describe the complex formation in pH regions II and III, because the points of the R=32, 16, and 8 complexes fall approximately on straight lines which yield positive intercepts as required by Eq. 16. From those graphic methods, however, no clear conclusion can be given on whether or not Scheme A is the correct one in pH region I. This is mainly because the unbound Cu^{2+} ion is almost undetectable in the high pH ($\geq$6) region, regardless of R, and also because the intervals between experimental points become narrow exceedingly as the pH becomes larger than about 5. These factors introduce large errors in the plots in Fig. 7.

From the logarithmic plots shown in Fig. 8, the values of K_1 and K_3 were estimated in pH regions II and III and are summarized in Table 2. It is interesting to note that the apparent dissociation constants, pK_1, of poly(Acr)–Cu(II) vary from pH region II to pH region III, as the R=8 and 16 plots indicate in Fig. 8. The

Table 2. The pK_1, $\log K_3$, and $\log (K_2 \cdot K_4)$ of Cu(II)–Acr complexes in poly(Acr)–Cu(II) at various R in pH regions II and III

	pH	II (Scheme B)		III (Scheme B)		II (Scheme C)	
		$\frac{pK_1}{\text{mol}\cdot\text{dm}^{-3}}$	$\frac{\log K_3}{(\text{mol}\cdot\text{dm}^{-3})^{-2}}$	$\frac{pK_1}{\text{mol}\cdot\text{dm}^{-3}}$	$\frac{\log K_3}{(\text{mol}\cdot\text{dm}^{-3})^{-2}}$	$\frac{pK_1}{\text{mol}\cdot\text{dm}^{-3}}$	$\frac{\log(K_2\cdot K_4)}{(\text{mol}\cdot\text{dm}^{-3})^{-2}}$
R	32	5.4	7.3	—	—	5.4	8.0
	16	5.5	7.2	5.1	6.8	5.5	7.9
	8	5.2	6.8	5.1	6.9	5.2	7.8

pK_1 values are in good agreement with those previously obtained for poly(Acr)–Cu(II) by the potentiometric titration method (4.91 in 0.2 M $NaNO_3$[5]) and 5—6 in 0.25 M $NaNO_3$[6])). The stability constants, $\log K_3$, are quite large as compared with those for Cu(II)–dicarboxylic acid complexes, suggesting a strong binding of Cu(II) to two carboxylato ligands of poly(Acr).

A slightly more complicated class of the binding reaction schemes involves four Acr residues per Cu(II). On the assumption that the four ligands are paired and each pair consists of two adjacent carboxylato groups of poly(Acr), the binding scheme may be written as

$$\text{Scheme C: } \mathrm{COOH} \overset{K_1}{\rightleftarrows} \mathrm{COO^-} + \mathrm{H^+},$$

$$\mathrm{(COO^-)_2} + \mathrm{Cu^{2+}} \overset{K_2}{\rightleftarrows} \mathrm{(COO)_2Cu},$$

$$\mathrm{(COO)_2Cu} + \mathrm{(COO^-)_2} \overset{K_4}{\rightleftarrows} \mathrm{[(COO)_2Cu(COO)_2]^{2-}} \tag{18}$$

The overall stability constant $K_2 \cdot K_4$ is then given as

$$K_2 \cdot K_4 = \frac{[\mathrm{Cu(COO)_4}^{2-}]}{[\mathrm{(COO^-)_2}]^2[\mathrm{Cu^{2+}}]}. \tag{19}$$

By combining K_1 and $K_2 \cdot K_4$, the following expression results:

$$\frac{2q((P_0/2)-2\beta)}{\sqrt{\sigma}} = \frac{[\mathrm{H^+}]}{K_1\sqrt{K_2 \cdot K_4}} + \frac{1}{\sqrt{K_2 \cdot K_4}}. \tag{20}$$

This expression is close to Eq. 16. The plots at three R values also give straight lines in pH region II similar to those in Fig. 8, when a value of 0.5 is again assumed for q throughout pH regions II and III (*cf.* Table 2). It should be noted then that the coordination of any two residues by a Cu(II), *i.e.*, Scheme B, can not be discriminated from the coordination of any two pairs of four residues by a Cu(II), *i.e.*, Scheme C, provided that each pair consists of two nearest neighbor carboxylato groups.

Discussion

The Absorption Spectra of Poly(Acr)–Cu(II) Macrocomplex. The UV-, near UV-, and visible bands have been reported for poly(Acr)- and poly(methacrylic acid)–Cu(II) systems.[2–4,8,10,12,15,16]) The UV- and visible bands are commonly observed in the Cu(II)-complexes with low molecular weight carboxylic acids of various types.[20,21]) The UV-band at 250 nm may be assigned to an allowed charge-transfer band between the carboxyl ligands of poly(Acr) and Cu(II) on the basis of its peak position and high intensity.[2,20]) The skewed visible band at 700 nm should be the d-d transition on the basis of its peak position and low absorption intensity.[10,15,20]) The skewed shape suggests the composite nature of this band, which should involve two or more d-d transitions.[20,22]) The existence of such multiple transitions was noted in the 860—890 nm region for the poly(methacrylic acid)–Cu(II) complex.[15])

Leyte *et al.*[15]) have observed the near UV-band at 380 nm in the poly(methacrylic acid)–Cu(II) system and suggested a binuclear Cu(II) complex of the acetate type by comparing their results with the studies of the Cu(II) complexes with acetate,[23]) unsaturated acid,[24]) and α,ω-dicarboxylic acid.[25,26]) However, the appearance of the near UV-band can not be considered as conclusive evidence of the binuclear Cu(II) complex.[21]) On the contrary, Graddon[27]) has assigned this band to the d_{xy}, $d_{yz} \to d_{x^2-y^2}$ transition of the planar, coordinated cupric ion from the results of the Cu(II)–acetylacetonate complex which has no dimeric structure. Hence, it is still unresolved whether or not the 370 nm band reflects the presence of the binuclear Cu(II) complex in poly(Acr)–Cu(II). This band appears even at a high ratio of the side-chain carboxyl groups to bound Cu(II) and is remarkable only in the low pH region III. Therefore, the Cu(II)–Acr complexes, which give rise to component spectra II and III (Fig. 6), could possibly be related structurally to the Cu(II)–acetylacetonate complex.

Structures of Cu(II)–Acr Complexes in Poly(Acr)–Cu(II) and Their Dependence on pH. The presence of three kinds of Cu(II)–Acr complexes in poly(Acr)–Cu(II) has been unraveled in the present work. However, it is not verified at present whether or not complexes, I, II, and III have unique structures. It is possible that each kind of complex i (i=I, II, III) is a mixture of several chemical species whose structures differ from each other slightly but do not affect the optical spectra appreciably. Figure 9 shows some of the likely chemical species for Cu(II)–Acr complexes. The structures of the species are by no means a complete list nor a conclusion introduced by this work, but should be considered as a working hypothesis. As regards the number of the ligands bound by a Cu(II), two carboxylato groups of poly(Acr) are normally considered because of the electric charge neutrality.[3,8,10]) As the remaining ligands to Cu(II), the solvent water, hydroxide ion, counter-ion ($\mathrm{Cl^-}$), and the additional carbonyl and carboxyl groups of poly(Acr) are all possible participants in the coordination with Cu(II), on the analogy of the Cu(II)–complexes with the small-molecular-weight ligands.[19–21]) The $\mathrm{Cl^-}$ ion may be discounted because the spectra of poly(Acr)–Cu(II)

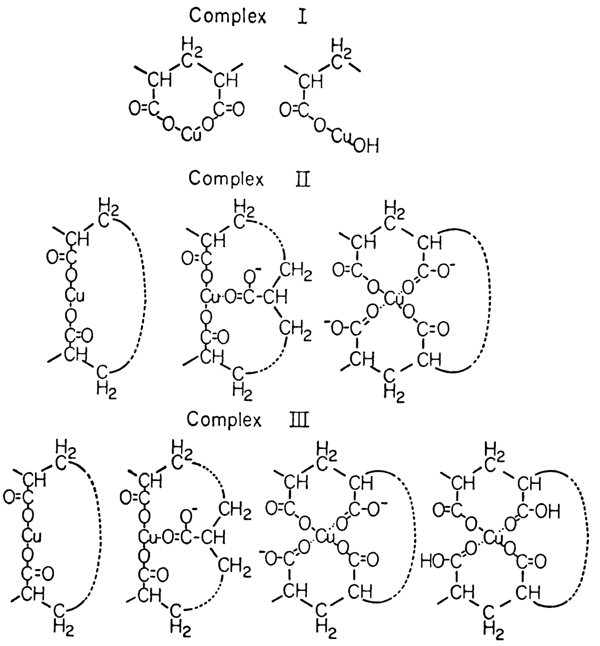

Fig. 9. Some possible structures of Cu(II)–Acr complexes in poly(Acr)–Cu(II). Neither hydration of water nor geometric isomer was explicitly considered. Complexes were assumed to be formed between Cu(II) and the side-chain carboxyl groups of a single poly(Acr) strand.

in 150 and 7.5 mM[2)] NaCl solutions show no essential differences.

Although the present data fail to confirm that the complex formation reaction involves the $[\mathrm{Acr}]^{-1}$-term in the high pH region (Scheme A), complex I is likely to be a bidentated-type complex, as already reported.[3,7)] Poly(Acr) is in a rather extended conformation in this pH region because of the charge repulsion, so that the Cu(II) may bind to a pair of nearest-neighbor carboxylato groups. Nevertheless, the binding of $\mathrm{Cu^{2+}}$ to a carboxylato groups and an $\mathrm{OH^-}$ ion could not be omitted. The complex formation reaction depends on the $[\mathrm{Acr}]^{-2}$-term (Scheme B) in the intermediate and low pH regions II and III where complexes II and III are dominant, respectively. This finding substantiates the notion that a bound Cu(II) is associated with the two carboxylato groups which are separated from, and independent of, each other on a single polymer strand (or possibly on different strands). The Cu(II) may also be coordinated by four carboxylato groups, as indicated by Scheme C. The profile of the component spectrum for complex II is very close to the spectrum of the Cu(II)–malonate complex which is also coordinated by four carboxylato groups (Fig. 6).[19)]

It is impossible at present to discriminate whether or not the chemical species for complexes II and III are formed between carboxylato groups of intra- or interchains. The poly(Acr)–Cu(II) complex may take on a compact or aggregated conformation, as the ionization of the side-chains is suppressed by the added protons. This view is supported by the remarkable decrease in the viscosity of poly(Acr) solutions in the presence of $\mathrm{Cu^{2+}}$ or $\mathrm{H^+}$.[8,10)] However, the bound Cu(II) can also bridge two polymer-strands by forming a planar, four-coordinated complex with two each out of four carboxylato groups (Scheme C). The overall conformation of the poly(Acr)–Cu(II) macro-ion should be studied by the light-scattering or sedimentation method to draw a definite conclusion on the role of the bound Cu(II) in the low pH regions.

The stability constants, in terms of $\log K_3$, of the Cu(II)–Acr complexes (*cf.* Table 2) are three to four orders of magnitude greater than the $\log K$ of Cu(II)–glutarate [3.16 (no salt),[28)] 3.88 (no salt), and 3.64 (in 0.2 M $\mathrm{NaNO_3}$)[5)]] and are comparable with those of Cu(II)–malonate and –oxalate complexes (*ca.* 8 and 5.54[5)]). Gregor *et al.*[5)] considered that the enormous electrostatic attraction of poly(Acr) toward $\mathrm{Cu^{2+}}$ contributes to the formation of a Cu(II)–Acr complex in poly(Acr) as stable as the Cu(II)–alkanoate complexes composed of five- and six-membered rings. However, it is also possible that the electrostatic repulsion is effectively suppressed in the presence of 150 mM NaCl and the conformation of poly(Acr) becomes either in the compact-coil or in the multi-stranded aggregates. The peculiar feature of the ligand field of the carboxyl groups of poly(Acr) toward the $\mathrm{Cu^{2+}}$ ion and the flexible backbone structure thereof may be the important cause to produce stable and large-ring Cu(II)–Acr complexes in poly(Acr).

Conclusion

The complicated pH dependence of the absorbance and peak position of the UV and visible absorption spectra of poly(Acr)–Cu(II) solutions was verified to be due partly to the dissociation of bound Cu(II) from the polymer sites in the low pH range (≤ 4.3), but mostly to the genuine variation of the spectra of the bound Cu(II) with pH. This variation with pH was interpreted as being due to the interplay of three component spectra characteristic of Cu(II)–Acr complexes I, II, and III. The fractions of complexes I, II, and III vary with pH, becoming most dominant in the high, intermediate, and low pH regions, respectively. The analysis of the binding reactions showed that the chemical species constituting those complexes involve both chelation and coordination of two to four side-chain carboxylato groups of poly(Acr). The present study strongly suggests the possibility that the bound Cu(II) also bridges two or more poly(Acr) strands to form multistrand aggregates.

References

1) Macromolecule–Metal Ion Complexes. V. For the preceding paper, see Ref. 2.

2) K. Yamaoka and T. Masujima, *Bull. Chem. Soc. Jpn.*, **52**, 1286 (1979).

3) F. T. Wall and S. J. Gill, *J. Phys. Chem.*, **58**, 1128 (1954).

4) A. M. Kotliar and H. Morawetz, *J. Am. Chem. Soc.*, **77**, 3692 (1955).

5) H. P. Gregor, L. B. Luttinger, and E. M. Loebl, *J. Phys. Chem.*, **59**, 34, 366, 559 (1955).

6) J. V. McLaren, J. D. Watts, and A. Gilbert, *J. Polym. Sci., Part C*, **16**, 1903 (1967).

7) P. Monjol, *Bull. Soc. Chim. Fr.*, **1972**, 1319.

8) K. Tamaoki, K. Imai, J. Nishino, and Y. Sakaguchi, *Kobunshi Kagaku*, **30**, 608 (1973).

9) J. A. Marinsky, N. Imai, and M. C. Lim, *Isr. J. Chem.*, **11**, 601 (1973).

10) H. Nishikawa and E. Tsuchida, *Bull. Chem. Soc. Jpn.*, **49**, 1545 (1976).

11) M. Mandel and J. C. Leyte, *J. Polym. Sci.*, **56**, S23 (1962).

12) M. Mandel and J. C. Leyte, *J. Polym. Sci.*, *Part A*, **2**, 2883, 3771 (1964).

13) R. L. Gustafson and J. A. Lirio, *J. Phys. Chem.*, **69**, 2849 (1965).

14) J. J. O'Neill, E. M. Loebl, A. Y. Kandanian, and H. Morawetz, *J. Polym. Sci.*, *Part A*, **3**, 4201 (1965).

15) J. C. Leyte, L. H. Zuiderweg, and M. van Reisen, *J. Phys. Chem.*, **72**, 1127 (1968).

16) J. A. Marinsky and W. M. Anspach, *J. Phys. Chem.*, **79**, 439 (1975).

17) S. Inoue, K. Yamaoka, and M. Miura, *J. Sci. Hiroshima Univ.*, *Ser. A*, **39**, 27 (1975).

18) K. Yamaoka and M. Masujima, *Biopolymers*, **17**, 2485 (1978).

19) D. P. Graddon, *J. Inorg. Nucl. Chem.*, **7**, 73 (1958).

20) D. P. Graddon, *J. Inorg. Nucl. Chem.*, **17**, 222 (1961).

21) M. Kato, H. B. Jonassen, and J. C. Fanning, *Chem. Rev.* **64**, 99 (1964).

22) R. Hirasawa and H. Kon, *J. Chem. Phys.*, **56**, 4467 (1972).

23) R. Tsuchida and S. Yamada, *Nature*, **176**, 1171 (1955).

24) B. J. Edmondson and A. B. P. Lever, *Inorg. Chem.*, **4**, 1608 (1965).

25) L. Dubicki, C. M. Harris, E. Kokot, and R. L. Martin, *Inorg. Chem.*, **5**, 93 (1966).

26) B. N. Figgis and D. J. Martin, *Inorg. Chem.*, **5**, 100 (1966).

27) D. P. Graddon, *J. Inorg. Nucl. Chem.*, **14**, 161 (1960).

28) J. M. Peacock and J. C. James, *J. Chem. Soc.*, **1951**, 2233.